

1 **Optimisation of 3D printed concrete for artificial reefs: biofouling**
2 **and mechanical analysis**

3 Océane Ly ^a, Adrian I Yoris-Nobile ^b, Nassim Sebaibi ^{a,*}, Elena Blanco-Fernandez ^b, Mohamed
4 Boutouil ^a, Daniel Castro-Fresno ^b, Alice E Hall ^c, Roger JH Herbert ^c, Walid Deboucha ^a,
5 Bianca Reis ^{d,e}, João N Franco ^{d,e}, Maria Teresa Borges ^{d,e}, Isabel Sousa-Pinto ^{d,e}, Pieter van der
6 Linden ^{d,e}, Rick Stafford ^c

7 ^a COMUE Normandie Université – Laboratoire Recherche Commun ESITC – ESITC Caen,
8 14610 Epron, France

9 ^b Universidad de Cantabria, 39005 Santander, Spain

10 ^c Bournemouth University, Poole, BH12 5BB, UK

11 ^d Faculdade de Ciências, Universidade do Porto, Rua do Campo Alegre s/n, 4150-181 Porto,
12 Portugal

13 ^e CIIMAR, Centro Interdisciplinar de Investigação Marinha e Ambiental, Terminal de
14 Cruzeiros do Porto de Leixões, Av. General Norton de Matos s/n, 4450-208 Matosinhos,
15 Portugal

16 *Corresponding author: nassim.sebaibi@esitc-caen.fr

17

18 **Abstract**

19 Protection, restoration, and regeneration of aquatic habitats are an increasingly important issue and are
20 requiring intensive research. In the marine environment, artificial reefs may be deployed to help offset
21 habitat loss, increase local biodiversity and stimulate the recovery of ecosystems. This study aimed at
22 the fabrication of artificial reefs by 3D printing. In the framework of the European INTERREG Atlantic
23 Area collaborative project “3DPARE”, six printed concrete formulations with limited environmental
24 impact, based on geopolymer or cement CEM III binders and recycled sands, were immersed in the
25 Atlantic along British, French, Portuguese and Spanish coasts. The colonisation of the concrete samples
26 by micro- and macroorganisms and their durability were assessed after 1, 3 and 6 months of immersion.
27 Results showed that both parameters were better with CEM III compared to geopolymer-based
28 formulations. Therefore the use of CEM III should be prioritised over these geopolymer binders in 3D
29 printed concrete for artificial reef applications.

30 *Keywords:* Artificial reef, 3D printing, Bio-receptive concrete, Geopolymer, Cement, Biofouling, Eco-
31 engineering

32 **1. Introduction**

33 Artificial reefs are man-made structures deployed on the seafloor with a history that goes as far as back
34 as the Roman Empire and Ancient Greece. Reefs were initially built for strategic military purposes such
35 as the blockade of harbours or the trapping of enemy ships [1]. Yet artificial reefs now serve more
36 specific objectives related to the restoration of fisheries and biodiversity and their deployment is often
37 aimed at mitigating the effects of resource exploitation including destructive practices such as trawling
38 [2]. Marine biodiversity provides beneficial ecosystem services such as commercial fisheries and
39 tourism, including recreational scuba diving [3], so conservation and restoration is an imperative.
40 Knowledge gained from the deployment of artificial reefs is also being applied to the ecological
41 enhancement of other coastal structures [4].

42 Evidence of artificial reef works dating from 1789 has been found in Japan [5] and in the USA during
43 the 19th century [6]. Their global deployment increased after World War II with the first national

44 programmes in Japan [7] and later to other continents [8]. In Europe, many private or public-funded
45 programmes were instigated in the Mediterranean Sea, however fewer have been deployed in the
46 Atlantic area due to high storm frequency and strong currents in the benthic zone that make it much less
47 stable and more difficult to study [9]. About 60 artificial reefs are listed in the OSPAR Maritime Area,
48 from Norway to Portugal [10], 25 of which being in Spanish territorial waters [11]. Reefs in this area
49 consist of car wrecks, shipwrecks, tyres and concrete blocks [12] [3] and geotextiles [13]. The design of
50 concrete reefs has been very simple as they were made by casting fresh concrete into formwork and, in
51 addition, the blocks were made of ordinary concrete [14]. Shapes varied from simple cubes or pipes
52 called Bonna, to more elaborated geometric structures called Typi and Babel, deployed in chaotic or
53 organised heaps, as seen on the French Atlantic coast [15]. First results of faunal monitoring studies on
54 the Aquitaine coast in France showed the major presence of benthic fishes around the artificial reefs
55 with higher taxa richness in more complex assemblies [16]. As complexity of design is important [12],
56 but difficult to attain with conventional fabrication methods, 3D printing of concrete is a recent and
57 promising technique which allows the design of very complex reefs (Fig. 1). In civil engineering, it
58 consists of the upward fabrication of structures by the deposition of successive layers of concrete slurry
59 with the help of a robotic arm or gantry. Debuts of 3D concrete printing for artificial reefs date from
60 2017 with projects in the Mediterranean Sea and in the Maldives.



61

62 **Fig.1.** 3D-printed artificial reefs submerged near Monaco coasts [17].

63 *Artificial Reef 3D Printing for Atlantic Area (3DPARE)* is a European project which gathers partners
64 from France, Portugal, Spain and the UK. It aims to design and then fabricate 3D printed artificial reefs
65 made of concrete to be deployed in the northern Atlantic area (Fig. 2). The first step was to optimise and

66 choose the concrete formulations to facilitate colonisation and provide shelter to small and large species.
67 The design aimed to be compatible with the marine environment, having less negative environmental
68 impact, and to be chemically and physically resistant to marine conditions and stable on site against
69 storms [18].



70 **Fig.2.** 3D-printed artificial reefs submerged

71 In the framework of 3DPARE project, these formulations are made from eco-friendly or recycled
72 materials including crushed seashell sand, glass sand or geopolymers as a binder. Geopolymer binder is
73 made of alumina-silicates, alkaline reagents such as sodium hydroxide NaOH or potassium hydroxide
74 KOH, and water. They release less carbon dioxide in the atmosphere upon fabrication than ordinary
75 Portland cement [19]. Other materials were also used, namely a ground granulated blast furnace slag
76 cement CEM III which has been commonly used by the Dutch for a century in marine applications [20],
77 and limestone sand.

78 While biofouling, *i.e.* the colonisation of wetted surfaces by biological microorganisms or
79 macroorganisms, is more often overlooked in the case of marine infrastructures deployment *i.e.* Dikes,
80 quay, etc – there is a large amount of literature on marine antifouling strategies. One major objective of
81 this work is to get the highest rate possible of biocolonisation and biodiversity.

82 **2. Experimental program**

83 **2.1. Materials used and sample preparation**

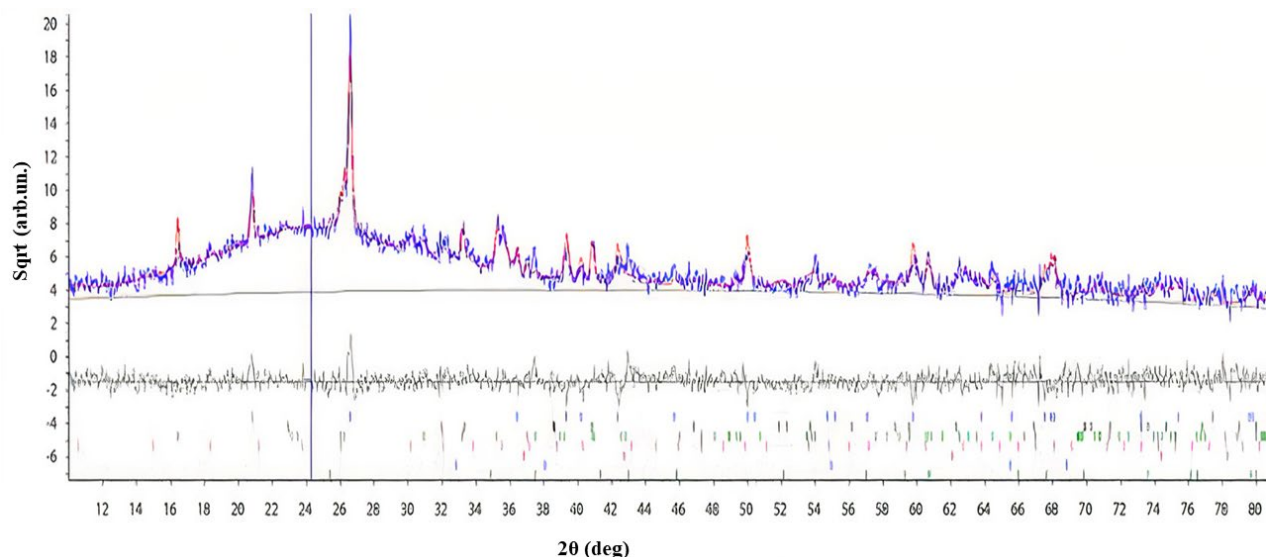
84 To manufacture artificial reefs by 3D printing, six formulations made with geopolymer and cement
85 mortars were analysed.

86 The terminology used for the identification of the formulations was the following: GL: geopolymer
87 mortar with limestone sand; GG: geopolymer mortar with 30% glass sand; GS: geopolymer mortar with
88 50% shell sand; CL: cement mortar with limestone sand; CG: cement mortar with 50% glass sand; CS:
89 cement mortar with 50% seashell sand.

90 The geopolymer mortars (GX) were manufactured with fly ash as the main binder; sodium hydroxide
91 (NaOH), tap water, additives, and limestone sand, glass sand and seashell sand, as fine aggregates. On
92 the other hand, cement mortars (CX) were manufactured with cement CEM. III/B 32.5 N-SR, tap water,
93 superplasticiser as additive, fly ash and kaolin as additions; and the same fine aggregates used for the
94 geopolymer mortars.

95 Fly ash was characterised by X-ray diffraction (XRD). For this, the ordinary range $10-80^\circ$ (2θ) with the
96 standard conditions for the diffractometer was explored working in the Bragg-Brentano configuration
97 with a copper tube with filtration of the radiation K_β ($\lambda = 1.5418 \text{ \AA}$). The estimate of the amorphous
98 contribution over the diffraction pattern was focused on $2\theta = 24.2^\circ$, compatible with the amorphous
99 phase of silicon oxide (SiO_2).

100 Fig. 3 shows the quantification of the possible crystalline phases, the most present being mullite
101 ($\text{Al}_{4+2x}\text{Si}_{2-2x}\text{O}_{10-x}$): 44.4%; quartz ($\alpha\text{-SiO}_2$): 23.4%; maghemite ($\gamma\text{-Fe}_2\text{O}_3$): 21.2%; magnetite (Fe_3O_4):
102 8.4%; and corundum (Al_2O_3): 2.0%. Loss of weight by calcination (LWC) was 2.4%.



103

104

Fig. 3. Relative percentages over the total of crystalline phases (% in weight).

105 NaOH in industrial form with initial molar concentration 25 M was employed after dilution in tap water
 106 to be used as an activator. The solution was prepared at least one day ahead of use.

107 Cement type III/B had an ordinary content of 31% clinker and 66% steel slag (data provided by the
 108 manufacturer). The physical properties of cement used are summarized in Table 1. MetaKaolin was
 109 analysed by X-ray fluorescence spectrometry and its composition was shown in Table 2.

110 **Table 1. Physical properties of cement**

Blaine fineness (cm ² /g)	28 days compressive strength (MPa)	Setting time (min)	
		Initial setting time	Final setting time
4500	44	210	265

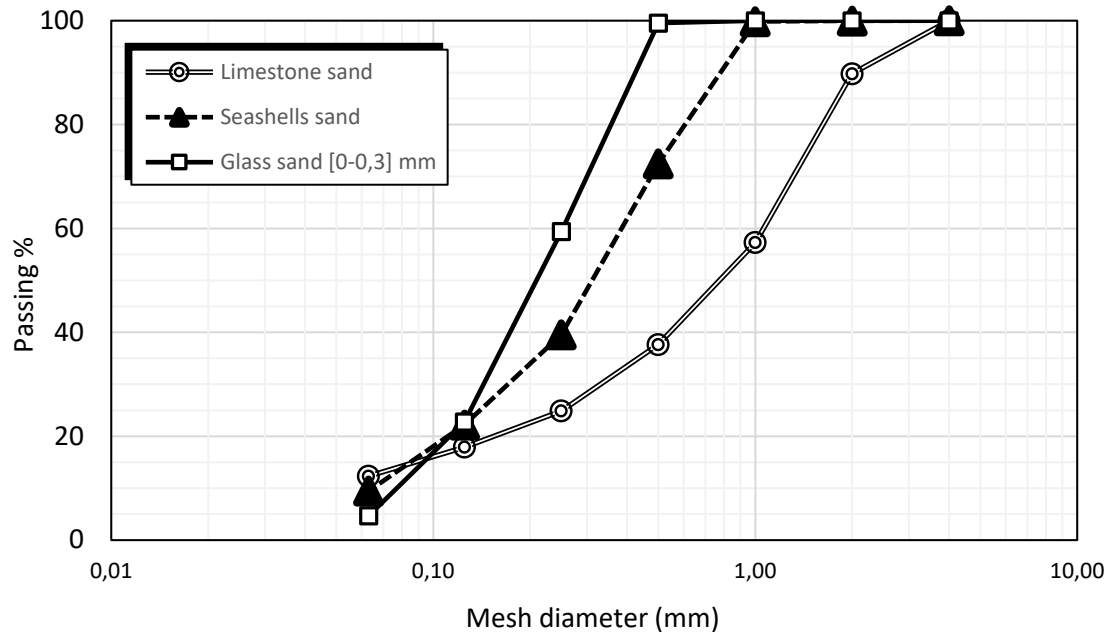
111

112 **Table 2.** Chemical composition of metakaolin (%)

SiO ₂	Al ₂ O ₃	Fe ₂ O ₃	CaO	MgO	Na ₂ O	K ₂ O	TiO ₂	LWC
48.3	35.5	1.5	0.24	0.4	0.1	1.35	0.28	12.5

113

114 Limestone sand, coming from quarry stone crushing, was provided in the fraction [0-3] mm. The crushed
 115 shells were obtained from the recycling of seashells coming from the canning industry. The glass came
 116 from smashed car windows in the fraction [0-0.3] mm. Fig. 4 represents the granulometric curves of the
 117 sands used in the mortars.



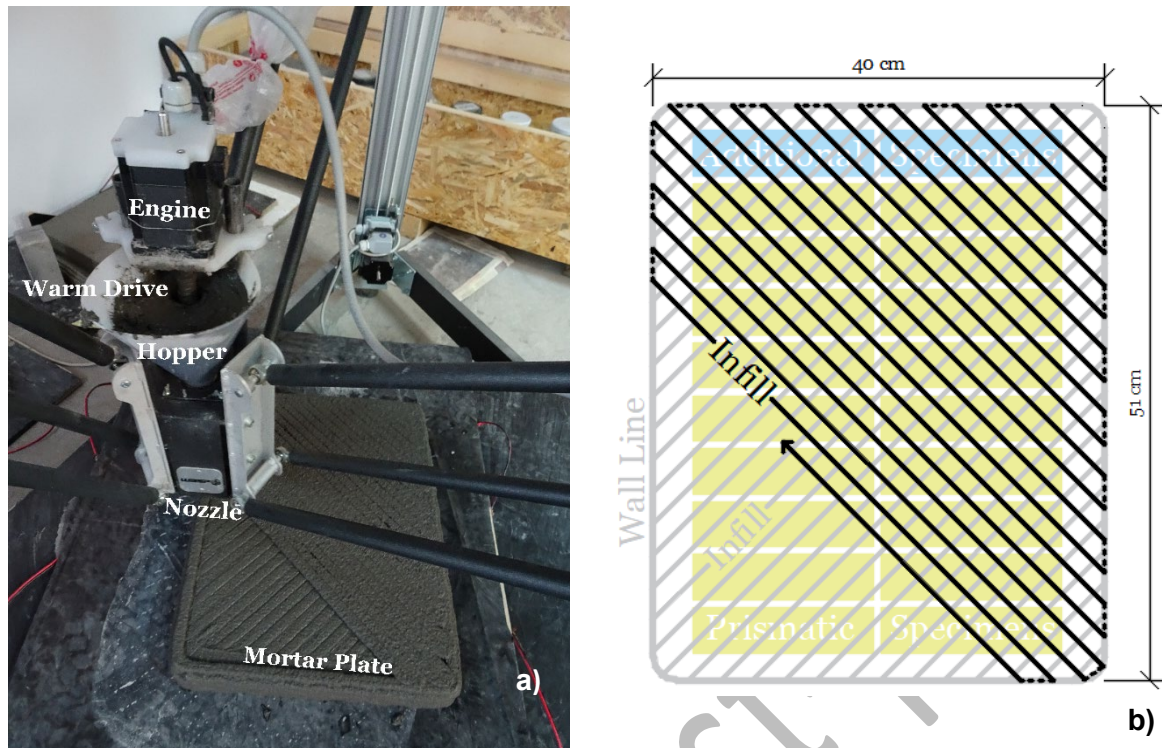
118

119

Fig. 4. Granulometric curves of the sands used in the mortars.

120 To carry out the experimental programme, $4 \times 4 \times 16$ cm prismatic specimens were fabricated with a
 121 3D printer type Delta of deposition per layer, whose maximal printing volume is 1 m diameter and 1 m
 122 height. The printer has a head which is composed of a hopper and a 3D worm drive inside, which, by
 123 spinning thanks to an electrical motor, drags the material to print towards the nozzle (Fig. 5a).

124 To obtain the prismatic specimens, mortar plates were printed with the 6 formulations under study,
 125 whose measurements were $40 \times 51 \times 6.4$ cm. The plate perimeter was printed with a wall line, while the
 126 area was filled with lines at 45° (with respect to the perimeter) which alternated layer after layer (Fig.
 127 5b). From each plate, 20 prismatic specimens were obtained, including two more than necessary in case
 128 any were damaged or there was any problem during sawing.



129 **Fig. 5.** a) 3D printer head details. b) Mortar plate printing and cutting scheme.

130 The distribution prismatic specimens was as follows: 4 partners (France, Spain, Portugal and United
 131 Kingdom); 6 different formulations; 5 immersion periods and one extra (1, 3, 6, 12, 24 months, extra);
 132 3 replicates per formulation. This led to a total of $432 + 108 = 540$ prismatic specimens.

133 The plates were printed with a nozzle of 20 mm diameter. A variable forward speed of the head of the
 134 printer was used, covering from 100 to 300 mm/s. The rotation speed of the worm drive to extrude the
 135 mortars was variable as well, going from 100 to 300 rpm.

136 From each plate, the required number of prismatic specimens by formulation was obtained for each
 137 partner. So, 6 mortar plates were fabricated per day, one plate for each formulation. In this way, the
 138 specimens corresponding to each partner were the same age.

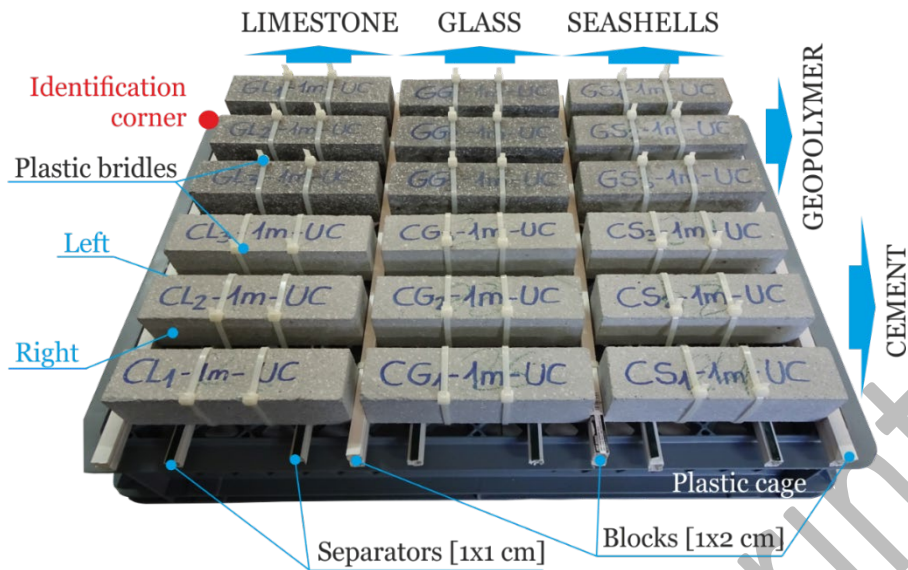
139 After 7-14 days, the prismatic specimens were cut from plates with a circular saw. The cutting process
 140 was carried out carefully so as not to mix the different mortars nor losing the printing orientation. Once
 141 the cutting was completed, the upper printing face of the prismatic specimens were identified. All
 142 mortars, both at the plate stage and also as prismatic specimens, were cured in air in a lab environment.

143 **2.2. Protocol of 3D printed samples immersion**

144 The specimens were printed in Spain and were consequently delivered to the other partners before they
145 were 28 days. For the delivery, the specimens were fully wrapped in bubble wrap and laid in plastic
146 boxes, to avoid damage. Upon arrival at destination, the bubble wrap was removed and the specimens
147 were left in air in a lab environment. The immersion was carried out when the specimens were around
148 70 days.

149 At each location, the 18 specimens (3 replicates of 6 formulations) were fixed to plastic platforms and
150 deployed in the sea. One platform was used for each age of immersion (in addition to an extra one set
151 in case there was a problem). This paper indicates the results of the specimens with immersion periods
152 of 1, 3 and 6 months, while those with periods of 12, 24 and extra are still immersed.

153 The platforms consisted of plastic boxes of 590 mm length, 365 mm width, 80 mm height and mesh
154 opening 20×20 mm. The boxes were inverted sideways to lay the specimens. Initially, plastic separators
155 with 1×1 cm of section were inserted between the box and the specimens; the specimens were placed
156 according to the order and distances shown in Fig.6. Specimens were set between blocks (1×2 cm of
157 section) to ensure that they could not move. Once the specimens were in place, they were fixed to the
158 boxes with plastic cable-ties of 4 mm width. The fastening of the samples was done in a way that allowed
159 the free circulation of seawater all around the samples.



160

161

Fig. 6. Arrangement of specimens on the platform.

162

The platforms with the specimens were immersed in the sea, separated by at least 1 m from the seabed and 1 m from the sea surface. Platforms were deployed in relatively sheltered locations to ensure that they did not swing in waves. All samples were immersed in the North-east Atlantic Ocean, off the coast of England (Poole Bay), France (Saint-Malo Bay), Portugal (Matosinhos Bay) and Spain (Santander Bay). Cages were removed at 1, 3 and 6 months of submersion.

166

167

2.3. Monitoring protocol for the characterisation survey and post deployment of pilot reefs surveys

168

169

The main objective of artificial reefs is to enhance the biodiversity of the deployment site. For this, they first have to attract microorganisms which will colonise the material and become one of the first links in the food chain. Attractiveness of the samples to marine life was measured by two means: first, the visual assessment of the biocolonisation of the samples by image processing, and second, the amount of biomass of the micro- and macroorganisms attached to the samples. The first method gives clues about the surface area that is colonised by organisms, whereas the second indicates the intensity of this colonisation. They thus provide complementary data on the bioreceptivity of the materials.

175

176

2.3.1. Visual assessment of biocolonisation by image processing

177 After the recovery of the samples at each time step, each of their sides (up, down, right, left) was
178 immediately scanned on arrival at the laboratory on a Canon Lide 300 office scanner (Canon, Japan)
179 with a 2400×4800 dpi resolution until the point at which they were colonised by macroorganisms. A
180 scanner was preferred to photographs as it ensured the same image quality for all partners in terms of
181 resolution, focal length or brightness. Scanned images were then processed on ImageJ (NIH, MD, USA)
182 open source software.

183 The protocol for the scanned images processing was as follows: 1) definition of the region of interest
184 (i.e. the samples boundaries) for each side; 2) 8-bit transformation of the raw image, assigning only grey
185 values to each pixel, from 0 (black pixel) to 255 (white pixel); 3) thresholding: this allows to make the
186 distinction between zones of interest (white colonised vs. black uncolonised); 4) computation of the
187 percentage of covering: this value was defined considering the mean grey values (Eq. 1) of the samples
188 following Eq. 2.

$$189 \text{ mean grey value} = \text{sum of each side's grey values} / \text{number of pixels} \quad (1)$$

$$190 \text{ covering percentage (\%)} = (\text{mean grey value} / 255) \times 100 \quad (2)$$

191 2.3.2. *Biomass of collected micro- and macroorganisms*

192 When scanning was performed, the entire surface of the samples was scrubbed manually with a brush
193 under distilled water in order to scrape off and collect all micro- and macroorganisms attached to the
194 samples. The water containing the biomass was then filtered on 25- μm filter papers which were weighed
195 after having being dried at 105 °C.

196 2.4. Mechanical tests

197 Mechanical tests were performed on the printed prismatic samples after the assessment of
198 biocolonisation procedure. For this, flexural strength, compressive strength and Young's modulus were
199 determined according to European standard EN 196-1, using an IGM 250 kN press (IGM, France), at
200 28 days of curing (reference properties), and at 1, 3 and 6 months after immersion. Briefly, a load of
201 0.05 kN/s was applied for the flexion test on the upper side of the whole prismatic sample according to

202 the printing direction, until failure. The obtained halves of each sample then underwent the compression
203 test on the same direction with a load of 2.4 kN/s. The Young's modulus was obtained measuring the
204 slope of the compression curve between 30 and 80% of the compressive strength where the curve is the
205 most linear.

206 **3. Results and discussion**

207 **3.1. Biocolonisation**

208 Biocolonisation and biomass results are summarised in Fig. 7 and 8, and Tables 3 to 5.

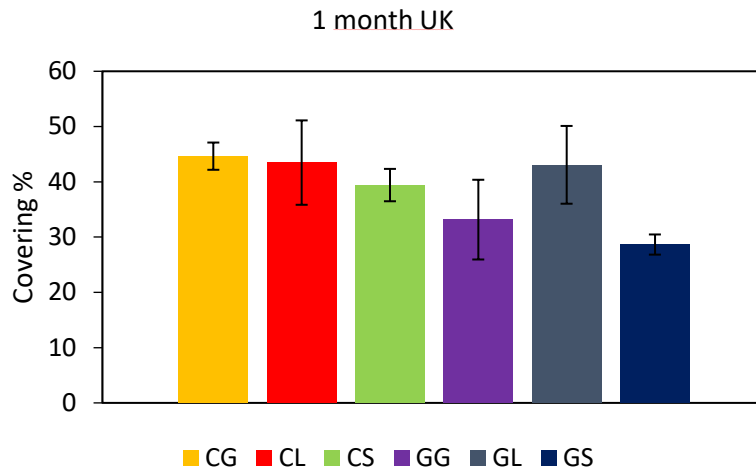
209 *3.1.1. Image processing*

210 Fig. 9 shows an example of raw scan image of one sample and the corresponding 8-bit and thresholded
211 equivalent. It should be noted that no scanning was performed for 3 and 6 months samples from England
212 and Portugal because of the presence of macroorganisms, as specified in the protocol mentioned in
213 Paragraph 2.3.1 (Fig. 10). A general observation was that all samples were colonised as indicated by a
214 noticeable change of colour (from grey and dark grey to brownish or greenish) However, biofouling was
215 different according to the immersion location. In fact, colonisation was much higher in the southern part
216 of the Atlantic (Portuguese and Spanish northern coasts) compared to its northern part (British and
217 French coasts). Results may appear mitigated, for samples – especially the French ones – for which the
218 colonisation was visually difficult to assess. For these, results were highly dependent on the eye and
219 discrimination capacity of the experimenter; however this bias was reduced by ensuring that all image
220 analyses were carried out by the same person. On the contrary, highly colonised samples – like
221 Portuguese and Spanish ones – were unequivocal.

222 UK 1 month results (Fig. 7a) showed that the best colonisation rates were observed for CG and CL with
223 a covering percentage of 44.6% and 43.8% respectively. CL is closely followed by GL with 43.1% of
224 the surface covered. A quite different rank was found for Portuguese 1 month samples (Fig. 7b),
225 dominated by CS (92.1%) followed by GS (87.4%) and CG (87.3%) on the last step. Here again, the
226 second and third best results are similar. With the French and the Spanish results at 1 month of
227 immersion (Fig. 8), it appears that generally, the best colonisation behaviour is observed for CX samples

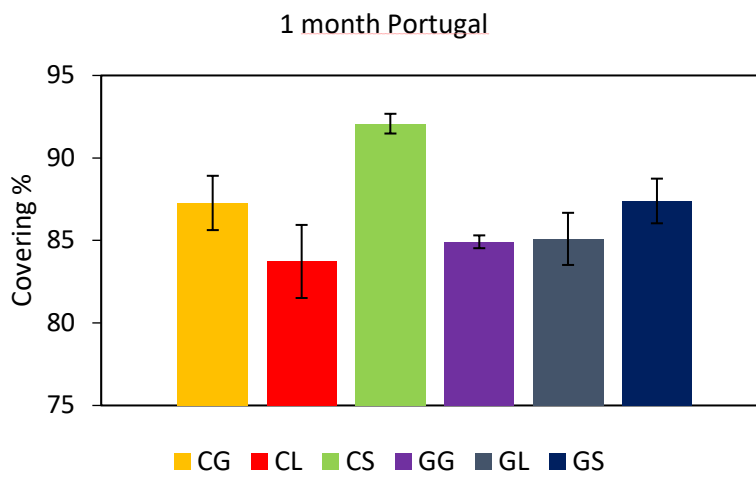
228 whereas it is less good with GX samples, though this is less true for Spanish 3 months results. The
229 hypothesis is that geopolymers leach high amounts of OH⁻ which affect the pH of the local habitat
230 (between 7.4 and 7.6 for seawater according to [21] and [22]), making it more alkaline. This release can
231 lead for some cases to a soaring pH of deionised water in a logarithmic trend from up to more than 10
232 in tens of minutes at 90 °C [23]. Yet a modification of pH to extremes – either basic or acid – is known
233 to be adverse to marine organisms. Indeed, pH can be used by potential basibionts (*i. e.* living organisms
234 as substrates) in their immediate vicinity as a chemical deterrent against epibionts (*i. e.* organisms living
235 on the surface of another living organism) in an antifouling defence strategy [24]. However, [25] showed
236 that the pH decreases slowly, from 11.3 to 10.2 on average up in 60 mL of distilled water over 28 days.
237 We can assume that the decrease of pH is more important in the large quantity of water represented by
238 the sea, and that dilution compensated the early “toxicity” of geopolymer towards microorganisms later
239 on. Portland blast furnace slag cement also leads to an increase of pH but the variation appears much
240 less important than with geopolymers, about 0.2 after 7 days in artificial seawater [26].

241 Despite those differences, we can see with the French and Spanish samples (Fig. 8) that all samples
242 follow the same trend, namely the tendency of the biofilm to cover the whole surface of the samples,
243 and we can assume that this is the same for the British and the Portuguese samples. In some way, it
244 supports the notion that all materials will be colonised to some extent, even if it were toxic on its surface
245 or by leaching, as claimed in the literature [27] [28]. Nevertheless, as they were tied to platforms with
246 cable ties which hide a small part of the available surface to colonisation accounting for uncolonised
247 zones, biofouling will never reach 100%.



248

a)



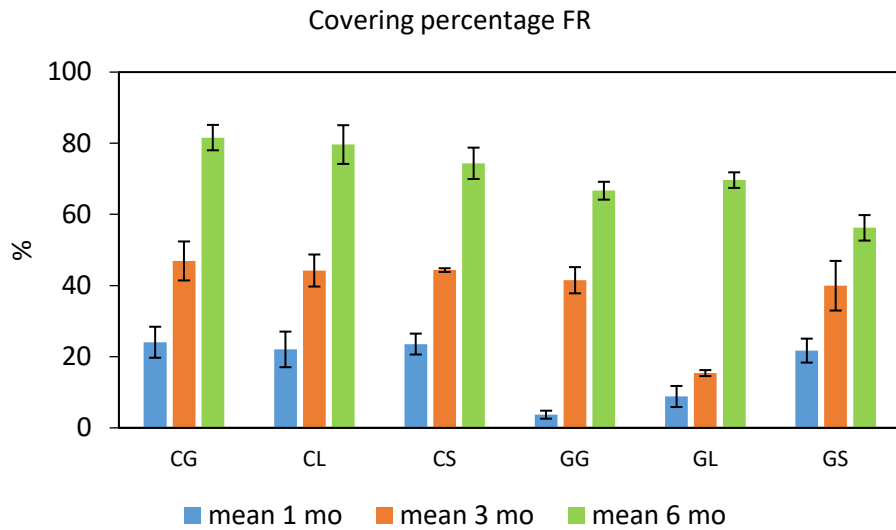
249

b)

250 **Fig. 7.** Mean biocolonisation coverage per material tested at 1 month, obtained from scanned images

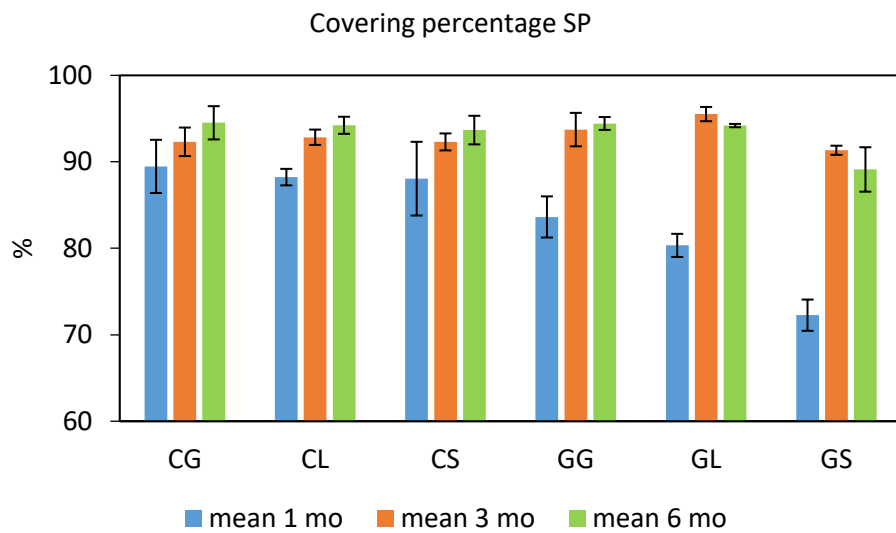
251

for a) the UK, b) Portugal.



252

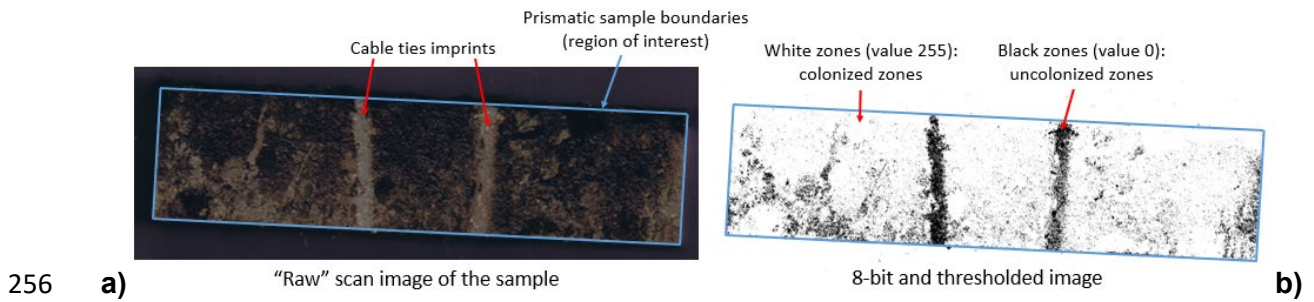
a)



253

b)

254 **Fig. 8.** Mean biocolonisation coverage per material tested at 1, 3 and 6 months, obtained from scanned
 255 images for a) France, b) Spain.



257 **Fig. 9.** Image processing: a) “Before” unprocessed scan image; b) “After” 8-bit and thresholded black
 258 and white image.



259
 260 **Fig. 10.** Example of sample partially covered with macroorganisms (mussels, ascidians). Samples with
 261 macroorganisms attached were not scanned, only biomass was measured.

262
 263 **3.1.2. Biomass**

264 Slightly higher values are observed on average with GX bricks compared to CX for 1 and 3 months
 265 (means of 1.74 g vs. 1.87 g and 8.1 g vs. 9.65 g respectively, Tables 3 and 4), but the association is
 266 reversed at 6 months of immersion (mean of 8.03 g for CX vs. 6.03 g for GX, Table 5). These differences
 267 vary from 0.13 g at 1 month to 2 g at 6 months. These values contrast with visual biocolonisation results

268 for which CX were generally superior ; it might indicate that the biofouling is more important and more
 269 localised for GX samples, while for CX samples the layer of biofouling is thinner but larger in surface
 270 area. Finally, we noted that, as for coverage, the collected biomass increased over time for all samples.
 271 This is due to the extended spreading of biofouling on the surface but also to the increase in thickness
 272 of the biological layer. This observation confirms the fact that once the first microorganisms are
 273 established, they can develop to their maximum stage of maturation. It is therefore promising for the
 274 attraction of macro species and the enhancement of the local habitat with more species and more
 275 individuals. Regional variation in biofouling coverage and biomass could be due to multiple abiotic
 276 factors, notably seawater temperature, turbidity and levels of nutrients including nitrates and phosphates.
 277 There is also the possibility of biological interactions such as the abundance of local grazers and
 278 predators.

279 **Table 3.** First month biomass dry weight data for materials tested in France (FR), the UK, Spain (SP)
 280 and Portugal (PT) and overall average.

1 month	FR [g]	UK [g]	SP [g]	PT [g]	AVERAGE [g]
CL	1.07	0.49	2.65	1.11	1.33
CS	0.67	0.34	2.57	1.07	1.16
CG	0.03	0.57	9.19	1.09	2.72
GL	0.02	0.72	5.06	1.24	1.76
GS	0.04	0.37	2.31	1.61	1.08
GG	0.79	0.37	8.48	1.41	2.76

281
 282 **Table 4.** Three months biomass dry weight data for materials tested in France (FR), the UK, Spain (SP)
 283 and Portugal (PT) and overall average.

3 months	FR [g]	UK [g]	SP [g]	PT [g]	AVERAGE [g]
CL	0.65	7.06	19.06	8.38	8.79
CS	0.63	5.95	14.09	10.28	7.74
CG	0.74	4.41	16.07	9.87	7.77
GL	0.99	4.62	22.63	9.77	9.50
GS	1.37	5.96	23.13	6.55	9.25
GG	1.08	5.86	19.32	14.53	10.20

284

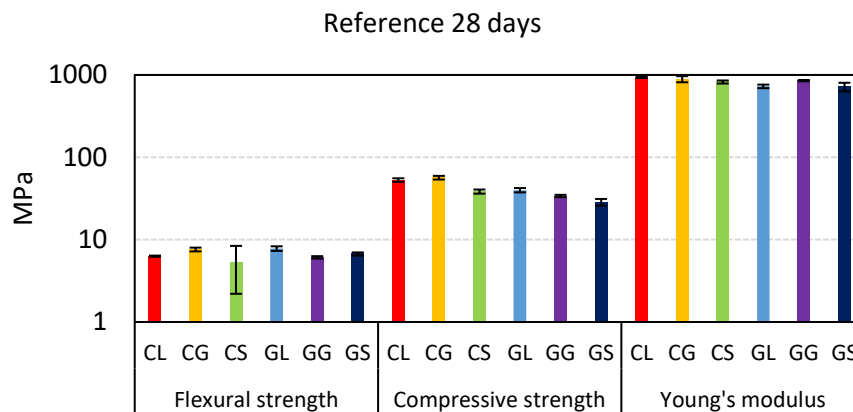
285 **Table 5.** Six months biomass dry weight data for materials tested in for France (FR), the UK, Spain (SP)
 286 and Portugal (PT) and overall average.

6 months	FR [g]	UK [g]	SP [g]	PT [g]	AVERAGE [g]
CL	1.78	5.91	8.20	17.89	8.44
CS	2.14	7.16	7.88	17.84	8.75
CG	1.91	5.94	9.93	9.80	6.89
GL	1.12	4.16	8.09	11.38	6.19
GS	1.90	4.23	8.85	9.73	6.18
GG	1.86	4.36	6.91	9.74	5.72

287

288 3.2. Mechanical results

289 Reference mechanical tests results obtained at 28 days of curing are presented in Fig. 11.

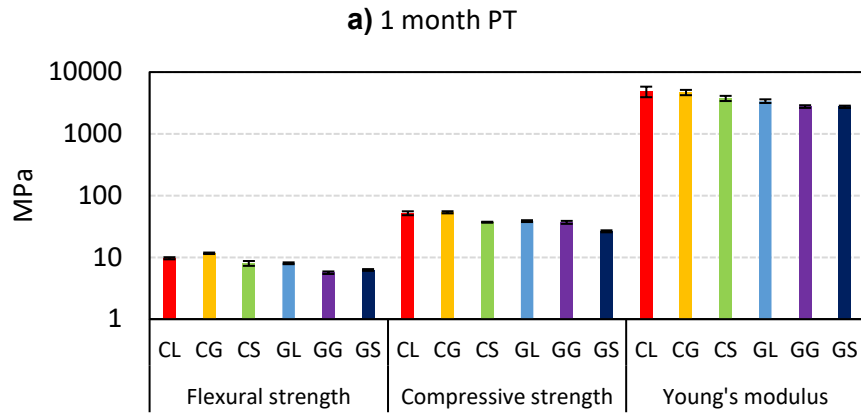


290

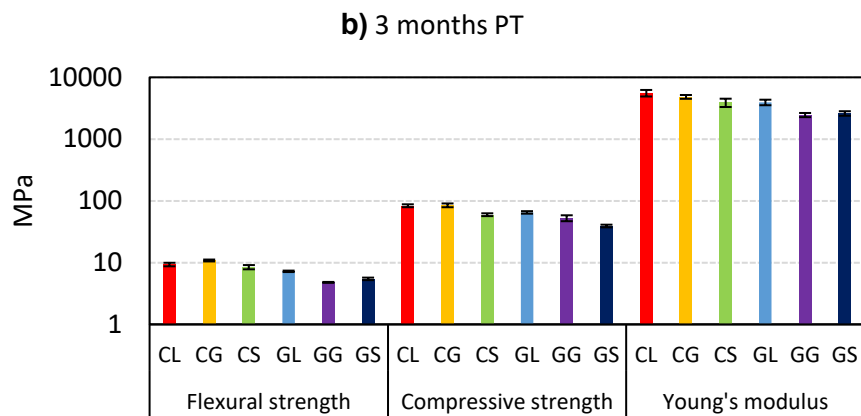
291 **Fig. 11.** Reference mechanical properties for tested materials at 28 days.

292 Mechanical tests results show the same trend over time, across all regions. Although different values
 293 were obtained from each region, the trend is similar for all three studied mechanical properties (flexural
 294 strength, compressive strength, Young's modulus). An example of what was observed for all regions is
 295 shown in Fig. 12. For each region and at each due time, even at 28 days, we observed better mechanical
 296 behaviour with CX samples than with GX except for GL which is comparable to CS.

297



298



299

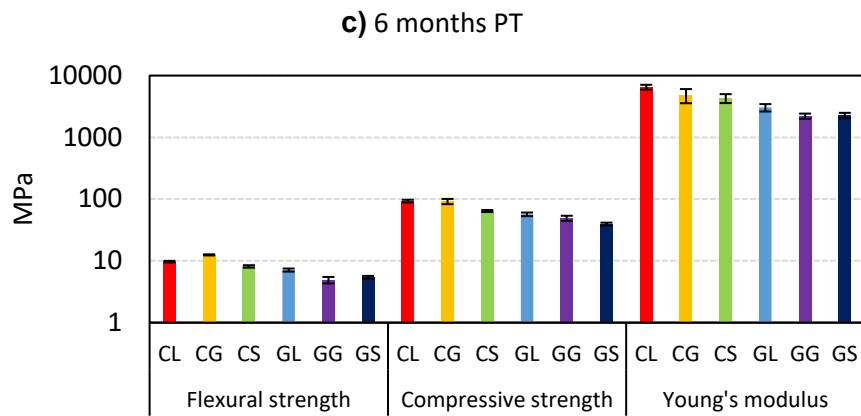
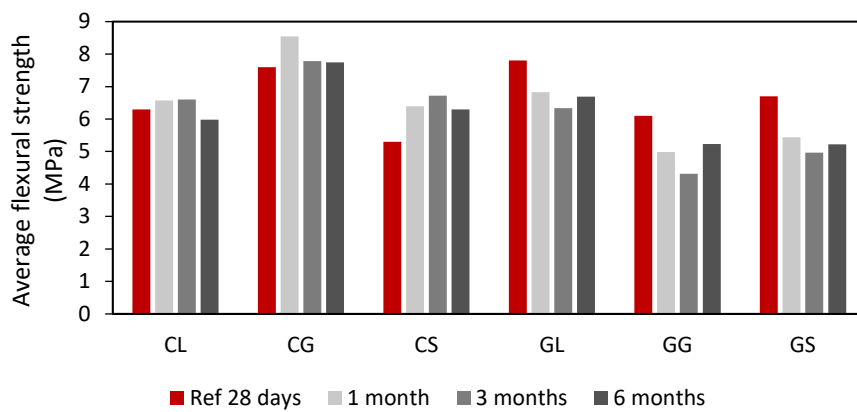


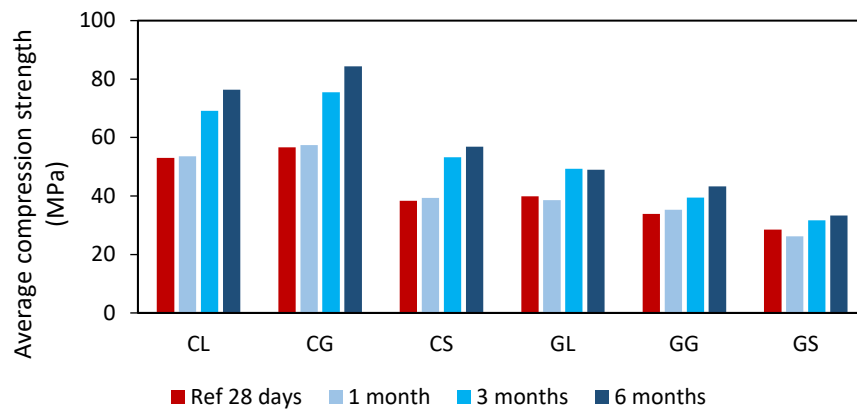
Fig. 12. Example of mechanical properties over time obtained for Portuguese samples at a) 1 month, b) 3 months, c) 6 months of submersion.

While averaging the mechanical properties values from all regions (Fig. 13), this association is even more clear, especially for the compressive strength and the Young's modulus with differences up to 50 MPa and 2 GPa respectively (CG vs. GS at 6 months). The flexural strengths are more alike and do not vary much over time compared to the other two mechanical properties. A major observation is the

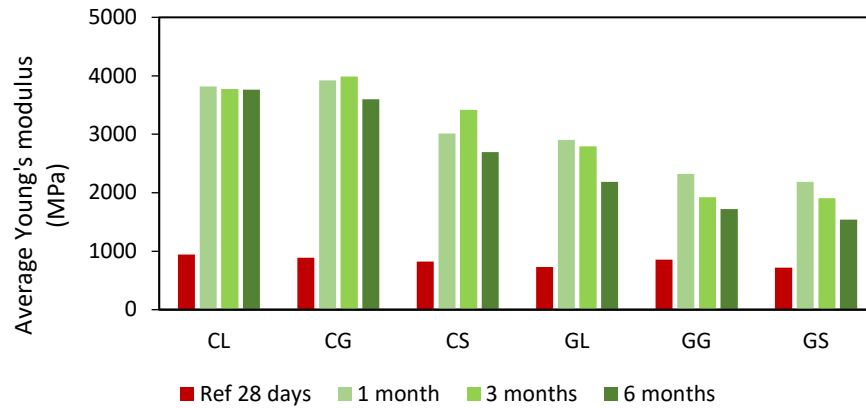
306 increase in compressive strength for both CX and GX, with a higher variation for CX. These results are
 307 consistent with the literature, as long term studies show that geopolymers can achieve 70% of their one-
 308 year compressive strength at 3 days, indicating a still-going geopolymerisation process [29]. This
 309 increase is slow [30] compared to CEM III the slow hydration process of which continues on the long
 310 term and highly contributes to the enhancement of ground granulated blast furnace slag cement
 311 performance. In fact, CEM III can achieve 128% of its 28-day strength at 180 days [31].



312 a)



313 b)



c)

314

315 **Fig. 13.** Overall average of mechanical properties of tested materials with submersion time: a) flexural
 316 strength, b) compressive strength, c) Young's modulus. Standard deviation is not represented as the
 317 values could differ a lot between regions . For one regions , it was small, like in Fig. 12.

318 Contrary to what is commonly accepted, the flexural strength may decrease as well as the elastic
 319 modulus, against the behaviour in compression, as seen here. This case has already been documented in
 320 [30] on geopolymers in seawater and can be encountered depending on the material characteristics
 321 (density, homogeneity, etc.). The same phenomenon might happen for cement in seawater. However, a
 322 low Young's modulus can be beneficial to slow down the propagation of cracks [30]. In addition, this
 323 behaviour was not strictly characteristic of all samples for one given region taken individually. Gererally
 324 the medium-term durability of all formulations was demonstrated here, with an advantage for CX. The
 325 biocolonisation might also have been an asset to protect the materials as it can be the case for other
 326 applications [32] [33].

327 4. Conclusion

328 The aim of this work was to assess the behaviour of 3D printable mortar formulations towards marine
 329 fauna and flora and their durability in seawater at medium term (1, 3 and 6 months). Both are major
 330 parameters to consider when designing artificial reefs. Yet further analysis should be undertaken and
 331 reported for the longer term deployments.

332

333 Mortar formulations with limited environmental impact composed of either geopolymers or cement CEM
334 III as binders and three kinds of sand were studied. Results showed that:

- 335 - Initial biocolonisation was better with CEM III compared to geopolymer-based formulations.
- 336 - However, both tend to reach the maximum colonisation rate.
- 337 - On average, mechanical properties were better with CEM III-based formulations over time.
- 338 - The trend was similar across regions.

339 Regarding biocolonisation and mechanical properties, initial results indicate that CEM III-based
340 formulations should thus be prioritised over geopolymer-based formulations for the 3D-printing of full-
341 scale artificial reefs. To date, the 12 and 24 months samples are still immersed and the monitoring of
342 their biocolonisation and durability continues.

343

344 **Acknowledgments**

345 The results presented in this article were obtained in the framework of the collaborative project *Artificial*
346 *Reef 3D Printing for Atlantic Area* (3DPARE), co-funded by the European Regional Development Fund
347 through the European cross-border programme INTERREG Atlantic Area.

348

349 **References**

- 350 [1] Hess RW, Rushworth D, Hynes MV, Peters JE. Disposal options for ships (No. RAND/MR-1377-
351 NAVY). RAND Corp Santa Monica CA; 2001.
- 352 [2] Crain CM, Halpern BS, Beck MW, Kappel CV. Understanding and managing human threats to the
353 coastal marine environment. *The Year in Ecology and Conservation Biology* 2009;1162:39-62.
- 354 [3] Baine M. Artificial reefs: a review of their design, application, management and performance. *Ocean*
355 *Coastal Manage* 2001;44:241-259.

- 356 [4] Firth LB, Knights AM, Bridger D, Evans AJ, Mieszkowska N, Moore PJ, O'Connor NE, Sheehan
357 EV, Thompson RC, Hawkins SJ. Ocean Sprawl: Challenges and opportunities for biodiversity
358 management in a changing world. *Oceanography and Marine Biology* 2016;54:193-269.
- 359 [5] Ino T. Historical review of artificial reef activities in Japan. In L Colunga and RB Stone (eds.),
360 *Proceedings of an international conference on artificial reefs* 1974;21-23.
- 361 [6] Stone RB. A brief history of artificial reef activities in the United States. In L Colunga and RB Stone
362 (eds.), *Proceedings of an international conference on artificial reefs* 1974;24-27.
- 363 [7] Thierry JM. Artificial reefs in Japan – A general outline. *Aquacult Eng* 1988;7:321-348.
- 364 [8] Lefevre JR, Duval C, Ragazzi M, Duclerc J. *Récifs artificiels : analyse bibliographique*; 1984.
- 365 [9] Barnabé G, Charbonnel E, Marinaro JY, Ody D, Francour P. Artificial reefs in France: analysis,
366 assessments and prospects. In AC Jensen et al. (eds.), *Artificial Reefs in European Seas* 2000;167-184.
- 367 [10] Fabi G, Spagnolo A, Bellan-Santini D, Charbonnel E, Çiçek BA, Goutayer García JJ, Jensen AC,
368 Kallianiotis A, Neves dos Santos M. Overview on artificial reefs in Europe. *Braz J Oceanogr*
369 2011;59(1):155-166.
- 370 [11] Jensen A. Artificial reefs of Europe: perspective and future. *ICES J Mar Sci* 2002;59:S3-S13.
- 371 [12] Bohnsack JA, Sutherland DL. Artificial reef research: a review with recommendations for future
372 priorities. *Bull Mar Sci* 1985;37(1):11-39.
- 373 [13] Herbert RJH, Collins K, Mallinson J, Hall AE, Pegg J, Ross K, Clarke L, Clements T. Epibenthic
374 and mobile species colonisation of a geotextile artificial surf reef on the south coast of England. *PLOS*
375 *One* 2017;12:e0184100.
- 376 [14] Pickering H, Whitmarsh D. Artificial reefs and fisheries exploitation: a review of the 'attraction
377 versus production' debate, the influence of design and its significance for policy. *Fish Res* 1997;31:39-
378 59.

- 379 [15] Tessier A, Francour P, Charbonnel E, Dalias N, Bodilis P, Seaman W, Lenfant P. Assessment of
380 French artificial reefs: due to limitations of research, trends may be misleading. *Hydrobiologia*
381 2015;753(1):1-29.
- 382 [16] Castège I, Milon E, Fourneau G, Tauzia A. First results of fauna community structure and dynamics
383 on two artificial reefs in the south of the Bay of Biscay (France). *Estuarine Coastal Shelf Sci*
384 2016;179:172-180.
- 385 [17] Boskalis Magazine (2018). 3D Printed Reefs. 15 March 2018.
- 386 [18] Lukens RR, Selberg C (project coordinators). Guidelines for marine artificial reef materials. Second
387 edition. A joint publication of the Gulf and Atlantic States Marine Fisheries Commission; 2004.
- 388 [19] Habert G, d'Espinose de Lacaillerie JB, Roussel N. An environmental evaluation of geopolymer
389 based concrete production: reviewing current research trends. *J Cleaner Prod* 2011;19:1229-1238.
- 390 [20] Polder RB, Nijland TG, de Rooij MR. Slag cement concrete – The Dutch Experience:
391 *Etatsprogrammet Varige konstruksjoner 2012-2015*; 2014.
- 392 [21] Marion GM, Millero FJ, Camões MF, Spitzer P, Feistel R, Chen CTA (2011). pH of seawater. *Mar*
393 *Chem* 2011;126:89-96.
- 394 [22] Halevy I, Bachan A. The geologic history of seawater pH. *Science* 2017;355(6329):1069-1071
- 395 [23] Aly Z, Vance ER, Perera DS, Hanna JV, Griffith CS, Davis J, Durce D. Aqueous leachability of
396 metakaolin-based geopolymers with molar ratios of Si/Al = 1.5—4. *J Nucl Mater* 2008;378(2):172-179.
- 397 [24] Wahl M. Marine epibiosis. I. Fouling and antifouling: some basic aspects. *Mar Ecol Prog Ser*
398 1989;58:175-189.
- 399 [25] Novais RM, Buruberry LH, Seabra MP, Bajare D, Labrincha JA. Novel porous fly ash-containing
400 geopolymers for pH buffering applications. *J Cleaner Prod* 2016;124:395-404.
- 401 [26] Matsunaga H, Tanishiki K, Tsuzimoto K. Environment-friendly block, “Ferroform”, made from
402 steel slag. *JFE GIHO* 2008;19:13-17.

- 403 [27] Dobretsov S, Abed RMM, Teplitski M. Mini-review: Inhibition of biofouling by marine
404 microorganisms. *Biofouling* 2013;29(4):423-441.
- 405 [28] McManus RS, Archibald N, Comber S, Knights AM, Thompson RC, Firth LB. Partial replacement
406 of cement for waste aggregates in concrete coastal and marine infrastructure: A foundation for ecological
407 enhancement? *Ecol Eng* 2018;120:655-667.
- 408 [29] Gunasekara C, Law DW, Setunge S. Long term permeation properties of different fly ash
409 geopolymer concretes. *Constr Build Mater* 2016;124:352-362.
- 410 [30] Olivia M. Durability related properties of low calcium flash ash based geopolymer concrete. PhD
411 thesis. Curtin University, Perth, Australia; 2011.
- 412 [31] Van Rompaey G. Étude de la réactivité des ciments riches en laitier, à basse température et à temps
413 court, sans ajout chloré. PhD thesis. Université Libre de Bruxelles, Brussels, Belgium; 2006.
- 414 [32] Shifler DA. Understanding material interactions in marine environments to promote extended
415 structural life. *Corros Sci* 2005;47:2335-2352.
- 416 [33] Lv J, Mao J, Ba H. Influence of marine microorganisms on the permeability and microstructure of
417 mortar. *Constr Build Mater* 2015;77:33-40.